"Eye and Vision Changes from Head Trauma"

Pathology of the Superior Colliculus in Chronic Traumatic Encephalopathy

Richard A. Armstrong D.Phil,[1] Ann C. McKee MD,[2,3] and Nigel J. Cairns PhD[4]

[1]Vision Sciences, Aston University, Birmingham B4 7ET, UK;

[2]Department of Pathology and Laboratory Medicine, VA Boston Healthcare System, Boston MA 01230 USA;

[3]Departments of Neurology and Pathology, Boston University School of Medicine, Boston, MA, 02118, USA;

[4]Departments of Neurology and Pathology & Immunology, Washington University School of Medicine, Saint Louis, Missouri 63110, USA.

Number of Tables: 4

Number of Figures: 6

Date submitted: 16 January 2016

Corresponding author: Dr. RA Armstrong, Vision Sciences, Aston University, Birmingham B4 7ET, UK (Tel: 0121-204-4102; Fax: 0121-204-3892; Email: R.A.Armstrong@aston.ac.uk)

Running Head: Pathology of superior colliculus in CTE

Abstract

Purpose: To investigate neuropathological changes in the superior colliculus (SC) in chronic traumatic encephalopathy (CTE).

Methods: The densities of the tau-immunoreactive neurofibrillary tangles (NFT), neuropil threads (NT), dot-like grains (DLG), astrocytic tangles (AT), and neuritic plaques (NP), together with abnormally enlarged neurons (EN), typical neurons (TN), vacuolation, and frequency of contacts with blood vessels were studied across the SC from pia mater to the periaqueductal gray (PAG) in eight CTE and six control cases.

Results: Tau-immunoreactive pathology was absent in the SC of controls but present in varying degrees in all CTE cases, significant densities of NFT, NT, or DLG being present in three cases. No significant differences in overall density of the NFT, NT, DLG, EN, vacuoles, or contacts with blood vessels were observed in control and CTE cases, but CTE cases had significantly lower mean densities of neurons. The distribution of surviving neurons across the SC suggested greater neuronal loss in intermediate and lower laminae in CTE. Changes in density of the tau-immunoreactive pathology across the laminae were variable but in six CTE cases, densities of NFT, NT, or DLG were significantly greater in intermediate and lower laminae. Pathological changes were not correlated with the distribution of blood vessels.

Conclusions: The data suggest significant pathology affecting the SC in a proportion of CTE cases with a laminar distribution which could compromise motor function rather than sensory analysis.

Key Words: Chronic traumatic encephalopathy (CTE), Superior colliculus, Neurofibrillary tangles (NFT), Neuronal loss, Laminar distribution

Introduction

Chronic traumatic encephalopathy (CTE) is a neurodegenerative disorder resulting from brain injury often accompanied by concussion.[1,2] It has been recorded in association with a variety of contact sports including boxing, American football, hockey, and wrestling[3] and also in military veterans exposed to blast shock waves from explosive devices.[4-7] Clinical symptoms of CTE include impairment of memory and executive function, behavioral change, and the presence of motor symptoms.[8]

Currently, CTE can only be diagnosed definitively using neuropathological criteria, cases exhibiting reduced gray matter volume in several brain regions, most prominently in frontal and anterior temporal lobes and associated with enlargement of the lateral and third ventricles.[5,9,10] Cases of CTE exhibit a complex histopathology in which the major feature is the formation of cellular aggregates in neurons and glia of the microtubule-associated protein (MAP) tau.[5,11] The neuronal pathology includes deposition of abnormal tau in the form of abnormal filaments, viz. neurofibrillary tangles (NFT) in frontal cortex,[11] temporal lobe, limbic system, and the striato-nigral system.[5] In addition, the pathology includes neuropil threads (NT) which may represent degenerating neurites and dot-like grains (DLG) which may represent synaptic structures. Abnormal aggregates of phosphorylated tau (ptau) may also occur in thorned astrocytes (AT).[8,9,10,11] The isoform profile and phosphorylation state of tau in CTE is similar to that of Alzheimer's disease (AD)[12] in that both three-repeat (3R) and four-repeat (4R) tau are present in equal ratios. Co-morbid AD neuropathologic

change (ADNC), viz., deposits of the protein beta-amyloid (Aβ) in association with neuritic degeneration termed neuritic plaques (NP).[13,14] In addition, abnormally enlarged neurons (EN), and vacuolation have been recorded in CTE as in other tauopathies.[15-17] Spatial correlations between tau pathology and blood vessels have also been reported suggesting dysfunction of the blood brain barrier (BBB) could be a factor in CTE.[5,9]

There is little available information on possible eye dysfunction relating directly to CTE. However, moderate to severe brain injury is associated with dysfunction of saccades and pursuits[18] and disconjugate eye movements especially affecting horizontal movement, have been recorded in 80% of individuals with concussion or blast injury.[19] The superior colliculus (SC) is a region of mid-brain involved in directing a behavioral response, via eye movements, towards a specific point or object.[20-22] It has a laminar structure consisting of seven layers (Fig 1), with alternating fiber-rich and cell-rich bands, the superficial layers (laminae I/II/III) being sensory in function and receiving input from the eyes and other sensory systems, while the deeper layers (laminae VI/VII) are motor-related and involved in the control of eye movements. The intermediate laminae (IV/V) are involved in both sensory and motor function. Tau-immunoreactive pathology has been observed in the SC in various neurodegenerative disorders including AD[23,24], corticobasal degeneration (CBD)[25], and progressive supranuclear palsy (PSP)[24] and in transgenic animal models of disease such as the 'tau-filament forming mice'[26] and in a triple mutation mouse model.[27] In addition, pathology in the SC in PSP results in 'slow vertical and horizontal saccades' or sequences of small amplitude saccades with preserved velocity.[28] Neuronal loss in the SC in Parkinson's disease (PD) also results in loss of

modulation which disturbs the balance between triggering and sustaining the input necessary for normal single-step saccades.[29] Hence, if there is tau pathology in the SC in CTE, it may give rise to possible eye movement dysfunction in the disorder. Hence, to test this hypothesis the densities of the tau-immunoreactive pathological changes, viz. NFT, NT, DLG, AT, NP together with EN, typical neurons (TP), vacuolation, and frequency of contacts with visible blood vessel profiles were studied across the SC in eight neuropathologically verified CTE cases and six controls. The study had the following objectives: (1) to determine whether there were quantitative differences in the pathology of the SC in neuropathologically diagnosed CTE cases and controls, (2) to determine whether the pathology was lamina specific, (3) to determine whether the pathological changes were correlated with the distribution of blood vessels, and (4) to consider how SC pathology might affect eye movements in CTE.

Materials and methods

Cases

Preserved samples of brain obtained at post-mortem of the CTE cases (N = 8, mean age 71 years, Range 61 – 82 years, SD = 6.94) (Table 1) were obtained from the Veterans Affairs – Boston University – Concussion Legacy Foundation ()VA-BU-CLF) Brain Bank. Control cases (N = 6, mean age 74 years, Range 64 – 83 years, SD = 8.21), with no neurological or psychiatric histories, with no recent evidence of brain trauma in medical records, and without ADNC (NIA-AA A0, B0)[30], were obtained from either the University of Birmingham Medical School or the Medical Research Council Neurodegenerative Disease Brain Bank, Department of Neuropathology,

Institute of Psychiatry, King's College London, UK. With the exception of one case, a boxer for 26 years (Case C), subjects with CTE had played American football with career durations ranging from 11-24 years. All CTE patients subjects had suffered at least one symptomatic concussion and multiple subconcussion episodes of trauma over the course of their careers. No eye movement or eye tracking tests were carried out on any subject during life. Cases were pathologically diagnosed with CTE according to NINDS criteria published by McKee et al.[10]: (1) foci of perivascular NFT, TA, and DLG irregularly distributed in cortex with a predilection for the sulcal depths, (2) NFT in superficial laminae II/III especially in temporal cortex, and (3) clusters of subpial AT in the cortex were present as an additional finding.

Histological methods

These studies were approved by the local Institute Review Board of Boston University and were carried out according to the 1995 Declaration of Helsinki (as modified in Edinburgh, 2000). After death, the next-of-kin provided written consent for brain removal and retention for research studies. Brains were fixed in 10% neutral buffered formalin for at least two weeks, paraffin-embedded, and sections cut at 6 μm. A section of the mid-brain was taken from each at the level of the third cranial nerve to study the SC. Sections were stained with luxol fast blue in combination with hematoxylin and eosin (LHE). In addition, immunohistochemistry was performed using an antibody against phosphorylated tau (AT8, Pierce Endogen, Rockford, IL, USA; 1:2000). Due to the rarity of brain material from neuropathologically verified CTE cases, all microscope slides were scanned and provided as ‘virtual slides’ using Aperio Image-Scope Software (Leica Biosystems Inc. Buffalo Grove, IL, USA).

Morphometric methods

The densities of the NFT, NT, DLG, AT, and NT together with EN, TN, vacuolation, and frequency of contacts with visible blood vessels was studied across the SC from pia mater to the periaqueductal gray (PAG). Two traverses were located at random normal to the laminar structure of the SC.[31] Random points were used for sampling rather than fixed locations to avoid sample bias attributable to pathology in the SC varying parallel to the pia mater. In all cases, 250 x 50 μm contiguous sample fields were superimposed over the image using either the draw or rectangle options. The sample fields were located along each traverse from the pia mater to the edge of the PAG. All histological features, with the exception of the blood vessel profiles, were counted within each sample field. NFT were present in the cytoplasm of larger cells with a distinct region of haematoxylin-positive cytoplasm (Fig 2) while AT were associated with larger, pale nuclei. NT were thread-like structures some of which were serpiginous, while small circular structures were identified as GR. Neurons with an abnormally enlarged perikaryon, a nucleus displaced to the periphery of the cell, and a cell diameter at least three times the nucleus diameter was counted as an EN.[32] TN were identified as cells containing at least some stained cytoplasm in combination with larger shape and non-spherical outline.[33] Additional structures can be identified in the sections including oligodendrocytes (small dark circular nuclei), astrocytes (larger light circular nuclei), and blood vessel profiles. The number of discrete vacuoles present in the neuropil greater than 5 μm in diameter, was also recorded.[34,35] To quantify blood vessel profiles in a sample field, a line was drawn across the long

dimension of the field at a random location and the number of contacts between the line and visible blood vessel profiles recorded.

Data analysis

Data analyses were carried out using STATISTICA software (Statsoft Inc., Tulsa, OK, 74104, USA). First, comparison of overall mean densities of a histological feature between CTE case and controls was made using 't' tests. Where no pathology was observed in controls, mean densities in CTE were compared to zero using a one-sample 't' test.[36] Second, the degree of degeneration present in the CTE cases made identification of the seven layers of the SC difficult. In addition, the pathology exhibited complex patterns of distribution across the SC rather than being confined to specific laminae. Hence, variations in density across the SC were analyzed using a polynomial curve-fitting procedure.[36,37] For each SC, polynomials were fitted successively to the data. Hence, quadratic curves are parabolic, cubic curves are 'S' shaped, and quartic curves often appear as 'double-peaked' or 'bimodal'. With each fitted polynomial, the correlation coefficients (Pearson's 'r'), regression coefficients, standard errors (SE), values of 't', and the residual mean square were obtained.[43]At each stage, the reduction in the sums of squares (SS) was tested for significance. The analysis was continued until either a non-significant value of F was obtained or there was little gain in the explained variance. To describe these distributions, the SC was divided into three zones: (1) an upper zone corresponding approximately to laminae I-III, (2) an intermediate zone corresponding to laminae IV and V, and (3) a lower zone corresponding to laminae VI and VII. Third, to determine whether densities of

histological features were spatially correlated with each other, and with blood vessels, correlations were tested using Pearson's correlation coefficient ('r').[38]

Results

The abundance of tau pathology in each of the eight CTE cases and a control cases are shown in Fig 3. In addition, overall densities of pathological changes in the SC of each CTE case are shown in Table 2. NFT, NT, and/or DLG were present in all cases, most significant densities being present in three cases (A, D and E) while two cases (B and H) had significantly less tau pathology. AT were present in 5/8 cases at relatively low density, NP were rare and present in only one case (A), and low densities of EN were present in 7/8 cases. In addition, vacuolation was present in all cases, with a mean density of 6.24 vacuoles per field (range 0.68 – 9.62). A comparison of overall mean densities of histological features in CTE and controls is shown in Fig 4. No tau-immunoreactive pathology was observed in control cases and mean densities of NFT, NT, DLG, and AT were not significantly different to zero. In addition, there were no significant differences in density of EN ($t = 0.60$, $P > 0.05$), vacuoles ($t = 0.84$, $P > 0.05$), or frequency of contacts with blood vessels ($t = 0.55$, $P > 0.05$) in CTE and controls. However, neuronal densities were significantly greater in the SC of control than CTE cases ($t = 3.76$, $P < 0.01$).

The distribution of the histological features across the laminae of the SC in each CTE case is shown in Table 3. First, in 4/8 cases, the density of NFT was significantly greater in intermediate and lower laminae, in 1/8 cases in upper laminae, and in 3/8 cases there were no significant changes in density across the SC. Second, in 3/5 and

5/7 cases respectively, NT and GR were predominantly located in intermediate and/or lower laminae. Third, in 2/2 cases and in 5/7 cases respectively, AT and EN exhibited no change in density across the SC. Fourth, in all cases, the densities of neurons were greatest in upper laminae, often declining significantly across the SC. Fifth, vacuoles were present with greater density in upper or upper and intermediate laminae in 7/8 cases. Sixth, changes in frequency of contacts with visible blood vessels were highly variable: in 3/8 cases there was no significant change across the SC, in 1/8 the vessels were most abundant in the intermediate laminae, a bimodal distribution was present in 3/8 cases, and in one case each, blood vessels were predominantly distributed in upper or intermediate laminae.

A comparison of the distribution of neurons across the SC in a typical control and CTE case is shown in Fig 5. The density of neurons in the control fluctuates across the SC, reflecting the alternating cell-rich and fiber-rich laminae, while the CTE case had significantly reduced numbers most marked in intermediate and lower laminae.

Spatial correlations among the densities of histological features are shown in Table 4. In five and four cases respectively, there were positive correlations between the NFT and NT and between NFT and GR consistent with the presence of these pathologies in the same laminae. In three cases, there was a positive correlation between the densities of GR and surviving neurons and in three cases between surviving neurons and vacuoles. Spatial correlation between the tau-immunoreactive pathology (NT) and the frequency of contacts with blood vessel profiles were present in only one case.

Discussion

Tau-immunoreactive pathology, mainly NFT, NT, and GR was present in the SC of all eight CTE cases studied, but with considerable variation among cases, overall densities not being significantly different from zero. However, three cases had significant densities of tau pathology, a further three cases had intermediate densities, while the remaining two cases had relatively low densities, desnity being unrelated to age or duration of career. EN and vacuoles were present in CTE but not at densities significantly different from controls. In addition, considerable differences in neuronal density were evident among CTE cases, but all cases had lower overall densities than the average of the controls. Hence, neuronal loss in the SC is present in all cases while a significant degree of tau pathology was also present in a proportion of cases suggesting the SC as a potential vulnerable site of CTE pathology.

Positive correlations were present among the densities of NFT, NT, and DLG, most notably between the NFT and NT/DLG suggesting a close spatial relationship between pathologies in the SC. This result supports the hypothesis that NFT, NT, and DLG could result from the degeneration of the same neurons, NFT aggregating in cell bodies and NT and DLG representing degeneration of adjacent neurites and synapses respectively.[39] In addition, the correlation between the density of DLG and TN in some cases supports the hypothesis that DLG could represent synaptic degeneration within the SC. The densities of the pathological changes across the SC were rarely correlated with the frequency of contacts with visible blood vessel profiles. This finding is consistent with previous observations showing that prominent perivascular fistribution of tau pathology in CTE is limited to cortical structures and not characteristic of midbrain or other brainstem regions.[5,9] Hence, the spread of tau

pathology among midbrain regions may be explained by the anatomical connections of the SC.[40]

Comparison of the changes in density of surviving neurons across the SC in CTE and control cases suggests significant neuron loss especially in intermediate and lower laminae in CTE. The superficial laminae of the SC receive projections mainly from the retina, cortical visual areas, pretectum, and the parabigeminal nucleus, the retinal input in particular enervating the entire superficial zone (Fig 6).[41] By contrast, the deeper layers also receive input from diverse sensory/motor areas, e.g., most cortical regions project to these laminae, and they also receive input from the substantia nigra, areas of the basal ganglia, spinal trigeminal nucleus, hypothalamus, zona incerta, thalamus, and inferior colliculus, some of which may also be affected in CTE. Pathological changes in the upper laminae could influence sensory analysis by the SC. By contrast, the deeper laminae send projections to many regions including the pulvinar and lateral intermediate thalamic nucleus which, in turn, send projections to cortical areas which control eye movement. In addition, the superficial laminae send projections to the pretectal nuclei, the lateral geniculate nucleus, and the parabigeminal nucleus. Projections from the deep nuclei are extensive with descending projections to brain stem and spinal cord and ascending projections to sensory/motor cortex involved in generating eye movements.[41]

In the majority of CTE cases, tau pathology and neuronal loss in the SC were more prominent in intermediate and lower laminae rather than the superficial laminae, and therefore, these changes could affect the process of directing eye movement via the oculomotor nucleus. These results contrast with those of Petras et al[42] in which rats

exposed to the effects of blast overpressure resulted in axonal degeneration in the SC principally affecting the superficial laminae II and III. However, none of our CTE cases examined had been exposed to blast damage and it is possible that laminar damage to the SC may be dependent on the type of brain injury. These findings suggest that eye movement abnormalities may be present in subjects with CTE and supports the suggestion that eye-tracking methodology might be useful as a diagnostic aid.[43,44]

In conclusion, the present study suggests neuronal loss in the SC is a consistent feature of CTE in addition to significant tau-immunoreactive pathological change in a proportion of cases. The distribution of the pathology together with that of surviving neurons across the SC, when compared with controls, suggests that anatomical connections involving the intermediate and lower laminae could be compromised in CTE. Hence, eye movement dysfunction is a possible clinical symptom associated with potential CTE cases. Future studies of concussion in athletes would benefit if athletes who agree to donate their brains on death would complete a comprehensive eye and binocular vision examination and pass those findings on to the appropriate neuropathology center.

Acknowledgements

The authors gratefully acknowledge the use of the resources and facilities at the Edith Nourse Rogers Memorial Veterans Hospital (Bedford, MA, USA). We also gratefully acknowledge the help of all members of the CTE center at Boston University School of Medicine, VA Boston and the Bedford VA, as well as the individuals and families

whose participation and contributions made this work possible. This work was supported by the National Institute of Neurological Disorders and Stroke (1UO1NS086659-01), Department of Veterans Affairs, the Veterans Affairs Biorepository (CSP 501), the Translational Research Center for Traumatic Brain Injury and Stress Disorders (TRACTS), Veterans Affairs Rehabilitation Research and Development Traumatic Brain Injury Center of Excellence (B6796-C), the National Institute of Aging Boston University Alzheimer's Disease Center (P30AG13846; supplement 0572063345–5). This work was supported by the Charles F. and Joanne Knight Alzheimer's Disease Research Center, Washington University School of Medicine, St. Louis, MO, USA (P50 AG05681 and P01 AG03991 from the National Institute on Aging). The authors have no associations, stock ownership, equity interests, patents, or licenses that could be perceived as a conflict of interest.

References

1. Jordan BD. The clinical spectrum of sport-related traumatic brain injury. Nat Rev Neural 2013;9:222-30.

2. Geddes J, Vowles G, Nicoll J, Revesz T. Neuronal cytoskeletal changes are an early consequence of repetitive brain injury. Acta Neuropathol 1999;98:171-78.

3. Maroon JC, Winkelman R, Bost J, Amos A, Mathyssek C, Miele V. Chronic traumatic encephalopathy in contact sports: A systematic review of all reported pathological cases. PLoS One 2015;10:e0117338.

4. Goldstein LE, Fisher AM, Tagge CA, ZhangXL, Velisek L, Sullivan JA, Upreti C, Kracht JM, Ericsson M, Wojmarowicj MW, et al. Chronic traumatic encephalopathy in blast-exposed military veterans and a blast neurotrauma mouse model. Sci Transl Med 2012;4:157lr5

5. McKee AC, Stein TD, Nowinski CJ, Stern RA, Daneshvar DH, Alvarez VE, Lee HS, Hall G, Wojtowicz SM, Baugh CM, et al. The spectrum of disease in chronic traumatic encephalopathy. Brain 2013;136:43-64.

6. McKee AC, Daneshvar DH, Alvarez VE, Stein TD. The neuropathology of sport. Acta Neuropathol 2014;127:29-51.

7. Shetty AK, Mishra V, Kodali M, Hattiangady B. Blood brain barrier dysfunction and delayed neurological deficits in mild traumatic brain injury induced by blast shock waves. Front Cell Neurosci 2014;8:Article No 232.

8. Saing T, Dick M, Nelson PT, Kim RC, Cribbs DH, Head E. Frontal cortex neuropathology in dementia pugilistica. J Neurotraum 2012;29:1054-70.

9. McKee AC, Stein TD, Kirenan PT, Alvarez VE. The neuropathology of chronic traumatic encephalopathy. Brain Pathol 2015;25:350-64.

10. McKee AC, Cairns NJ, Dickson DW, Folkerth RD, Keene CD, Litvan I, Perl D, Stein TD, Vonsattel JP, Stewart W, et al. The first NINDS/NIBIB consensus meeting to define neuropathological criteria for the diagnosis of chronic traumatic encephalopathy. Acta Neuropathol 2016;131:75-86.

11. Kieman PT, Montinegro PH, Solomon TM, McKee AC. Chronic traumatic encephalopathy: A neurodegenerative consequence of repetitive brain injury. Semin Neurol 2015;35:20-8.

12. Schmidt M, Zhukareva V, Newell K, Lee V, Trojanowski J. Tau isoform profile and phosphorylation state in dementia pugilistica recapitulate Alzheimer's disease. Acta Neuropathol 2001;101:518-24.

13. Graham DI, Gentleman SM, Lynch A, Roberts GW. Distribution of beta-amyloid protein in the brain following severe head-injury. Neuropath Appl Neurobiol 1995;21:27-34.

14. Johnson VE, Stewart W, Smith DH. Widespread tau and amyloid-beta pathology many years after a single traumatic injury in humans. Brain Pathol 2012;22:142-9.

15. Armstrong RA, Cairns NJ, Lantos PL. Quantification of pathological lesions in the frontal and temporal lobe in ten patients diagnosed with Pick's disease. Acta Neuropathol 1999;19:64-70.

16. Armstrong RA, Cairns NJ, Lantos PL. A quantitative study of the pathological lesions in the neocortex and hippocampus of 12 patients with corticobasal degeneration. Exp Neurol 2000;163:348-56.

17. Armstrong RA, Lantos PL, Cairns NJ. Progressive supranuclear palsy (PSP): a quantitative study of the pathological changes in cortical and subcortical regions of eight cases. J Neural Transm 2007;114:1569-77.

18. Ventura RE, Balcer LJ, Galetta SL. The neuro-ophthalmology of head trauma. Lancet Neurol 2014;13:1006-16.

19. Samadani U, Ritiop R, Reyes M, Nehrbass E, Li M, Lamm E, Schneider J, Shimunov D, Sava M, Kolecki R, et al. Eye tracking disconjugate eye movements associated with structural traumatic brain injury and concussion. J Neurotraum 2015;32:548-56.

20. Kustov A, Robinson D. Shared neural control of attentional shifts and eye movements. Nature 1996;384:74-7.

21. Sprague JM. Neural mechanisms of visual orienting responses. Prog Brain Res 1996;112:1-15.

22. Klier E, Wang H, Crawford D. Three-dimensional eye-head coordination is implemented downstream from the superior colliculus. J Neurophysiol 2003;89:2839-53.

23. Leuba G, Saini K. Pathology of subcortical visual centers in relation to cortical degeneration in Alzheimer's disease. Neuropath Appl Neurobiol 1995;21:410-422.

24. Dugger BN, Tu M, Murray ME, Dickson DW. Disease specificity and pathological progression of tau pathology in brainstem nuclei of Alzheimer's disease and progressive supranuclear palsy. Neurosci Lett 2011;491:122-126.

25. Hattori M, Hashizume Y, Yoshida M, Iwasaki Y, Hishikawa N, Ueda R, Ojika K. Distribution of astrocytic plaques in corticobasal degeneration brain and comparison with tuft-shaped astrocytes in the progressive supranuclear palsy brain. Acta Neuropathol 2003;106:143-149.

26. Morcinek K, Kohler C, Gotz J, Schroder H. Pattern of tau hypephosphorylation and neurotransmitter markers in the brainstem of senescent tau forming transgenic mice. Brain Res 2013;1497:73-84.

27. Overk CR, Kelley CM, Mufson EJ. Brainstem Alzheimer's-like pathology in the triple transgenic mouse model of Alzheimer's disease. Neurobiol Dis 2009;35:415-425.

28. Terao Y, Fukuda H, Shirota Y, Yugeta A, Yoshioka M, Suzuki M, Hanajima R, Nomura Y, Segawa M, Tsuji S, et al. Deterioration of horizontal saccades in progressive supranuclear palsy. Clin Neurophysiol 2013;124:354-363.

29. Keller EL, Lee BT, Lee KM. Frontal eye field signals that may trigger the brainstem saccade generator. In: Using eye movements as an experimental probe in brain function-A symposium in honor of Jean Buttner-Ennever. Progress in Brain Research 2008;171:107-114.

30. Hyman BT, Phelps CH, Beach TG, Bigio EH, Cairns NJ, Carrillo MC, Dickson DW, Duyckaerts C, Frosch MP, Masliah E, et al. National Institute on Aging-Alzheimer's Association guidelines for the neuropathologic assessment of Alzheimer's disease. Alz Dement 2012;8:1-13.

31. Duyckaerts C, Hauw JJ, Bastenaire F, Piette F, Poulain C, Rainsard V, Javoy-Agid F, Berthaux P. Laminar distribution of neocortical senile plaques in senile dementia of the Alzheimer type. Acta Neuropathol 1986;70:249-56.

32. Armstrong RA. A quantitative study of abnormally enlarged neurons in cognitively normal brain and neurodegenerative disease. Clin Neuropathol 2013;32:128-34.

33. Armstrong RA. Correlations between the morphology of diffuse and primitive β-amyloid (Aβ) deposits and the frequency of associated cells in Down's syndrome. Neuropath Appl Neurobiol 1996;22:527-30.

34. Armstrong RA, Ironside J, Lantos PL, Cairns NJ. A quantitative study of the pathological changes in the cerebellum of 15 cases of variant Creutzfeldt-Jakob disease. Neuropathol Appl Neurobiol 2009;35:36-45.

35. Armstrong RA, Lantos PL, Cairns NJ. Spatial correlations between the vacuolation, prion protein deposits, and neurons in the cerebral cortex in sporadic Creutzfeldt-Jakob disease. Neuropathology 2001;21:266-71.

36. Snedecor GW, Cochran WG. *Statistical Methods*. Iowa State University Press, Ames, Iowa USA, 1980.

37. Armstrong RA, Hilton AC. *Statistical Analysis in Microbiology: Statnotes.* Wiley Blackwell, Hoboken, New Jersey, 2011.

38. Armstrong RA. Measuring the degree of spatial correlation between histological features in thin sections of brain tissue. Neuropathology 2003;23:245-53.

39. Armstrong RA, Kotzbauer PT, Perlmutter JS, Campbell MC, Hurth KM, Schmidt RE, Cairns NJ. A quantitative study of α-synuclein pathology in fifteen cases of dementia associated with Parkinson disease. J Neural Transm 2014;121:171-81.

40. Goedert M, Clavaguera F, Tolnay M. The propagation of prion-like protein inclusions in neurodegenerative diseases. Trends Neurosci 2010;33:317-25.

41. Brodal A. Neurological Anatomy. 3rd ed. Oxford: Oxford University Press, 1981.

42. Petras JM, Bauman RA, Elsayed NM. Visual system degeneration induced by blast overpressure. Toxicology 1997;121:41-49.

43. Galetta KM, Barrett J, Allen M, Madda F, Delicate D, Tennant AT, Branas CC, Maguire MG, Messner LV, Devick S, et al. The King-Devick test as a determinant of head trauma and concussion in boxers and MMA fighters. Neurology 2011;76:1456-62.

44. Leong DF, Balcer LJ, Galetta SL, Liu Z, Master CL. The King-Devick test as a concussion screening tool administered by sports parents. J Sports Med Phys Fitness 2014;54:70-7.

Table 1. Demographic features, frequency of traumatic incidents, and sporting career length of the eight chronic traumatic encephalopathy cases studied.

Case	Onset (yrs)	Severity score	Duration (yrs)	Death (yrs)*	Trauma	Career length (yrs)
CTE						
A	65		10	75	10/2	18	4
B	66		4	70	10/1	11	4
C	55		6	60	1/1	26	3
D	56		10	65	-	19	3
E	67		15	80	F	12	4
F	38		40	80	-	18	3
G	55		11	65	50/1	17	3
H	45		26	70	F	20	4
Control							
A	-		-	64	-	-	-
B	-		-	65	-	-	-
C	-		-	72	-	-	-
D	-		-	80	-	-	-
E	-		-	83	-	-	-
F	-		-	80	-	-	-

In column 5 of CTE cases: first figure is frequency of reported traumatic episodes, second figure, episodes resulting in loss of consciousness. Abbreviations: F = frequent, (-) = data not available, * Age of CTE cases rounded to nearest 5-year age interval to protect subject identities).

Table 2. Mean densities (50 x 250μm sample field) of histological features in the superior colliculus of eight cases of chronic traumatic encephalopathy.

	Histological feature								
Case	NFT	NT	DLG	AT	EN	N	V	NP	BV
A	1.18	10.50	22.61	0.39	0.16	11.06	5.24	0.04	0.45
B	0.21	0	0.03	0	0.15	8.85	0.68	0	0.68
C	0.34	0.31	0.93	0.24	0.24	4.72	0.93	0	0.93
D	3.0	0.27	9.09	0.02	0.50	8.07	2.84	0	0.61
E	1.11	0.32	3.43	0.04	0.09	7.37	3.89	0	0.87
F	0.30	0.08	0.22	0	0	2.05	9.62	0	0.38
G	0.12	0.12	0.63	0.07	0.14	5.88	7.35	0	0.33
H	0.09	0.07	0.12	0	0.30	7.0	4.16	0	0.47
Mean control	0	0	0	0	0.15	16.43	6.14	0	0.65
SE					(0.01)	(0.83)	(0.66)		(0.14)

Data for BV are frequency of contacts of a randomly drawn line across the field with visible BV profiles. Abbreviations**:** NFT = Neurofibrillary tangles, NT = Neuropil threads, DLG = Dot-like grains, AT = Astrocytic tangles, EN = Enlarged neurons, N = Neurons, V = Vacuoles, NP = Neuritic plaques, BV = Blood vessels, SE = Standard error of mean

Table 3. Distribution of the histological features across the superior colliculus in eight cases of chronic traumatic encephalopathy.

	Histological feature								
Case	NFT	NT	DLG	AT	EN	N	V	NP	BV
A	I,L	I,L	I,L	NS	NS	U	IL	L	I
B	NS	-	-	-	NS	U	U	-	Bi
C	I,L	NS	NS	NS	NS	U	U	-	NS
D	I,L	I,L	I,L	-	L	U	U	-	Bi
E	NS	I,L	I,L	-	I,L	U	U	-	NS
F	U	-	U	-	-	U	U	-	NS
G	NS	NS	L	-	NS	U	U	-	Bi
H	I,L	-	I,L	-	NS	U	U,I	-	U

The table shows the region of the SC with highest densities of a particular histological feature. Abbreviations: NFT = Neurofibrillary tangles, NT = neuropil threads, DLG = Dot-like grains, AT = Astrocytic tangles, EN = Enlarged neurons, N = neurons, V = vacuoles, BV = Blood vessels U = Upper laminae, I = Intermediate laminae, L = Lower laminae, Bi = Bimodal distribution, NS = No significant change with density across the SC, (-) = Insufficient density to determine laminar distribution

Table 4. Summary of the spatial correlations (Pearson's 'r') of the histological features across the superior colliculus in eight cases of chronic traumatic encephalopathy.

	Histological features							
	NFT	NT	DLG	AT	EN	N	V	BV
NFT	-	5,0	4,0	0	2,0	2,0	1,1	0
NT		-	2,0	0	0	1,0	0,1	1,0
DLG			-	0	0	3,0	1,2	0
AT				-	0	0	0	0
EN					-	0	0	0
N						-	3,1	0,1
V							-	1,0
BV								-

First and second figures are number of cases with positive and negative correlations respectively. Abbreviations: NFT = Neurofibrillary tangles, NT = Neuropil threads, DLG = Dot-like grains, AT = Astrocytic tangles, EN = Enlarged neurons, N = Neurons, V = Vacuoles, BV = Blood vessels

Legends to figures

Fig 1. Section through the superior colliculus (SC) showing the approximate location of the seven laminae (I – VII); PAG = Periaqueductal gray; luxol fast blue in combination with hematoxylin and eosin (LHE), bar = 1 mm.

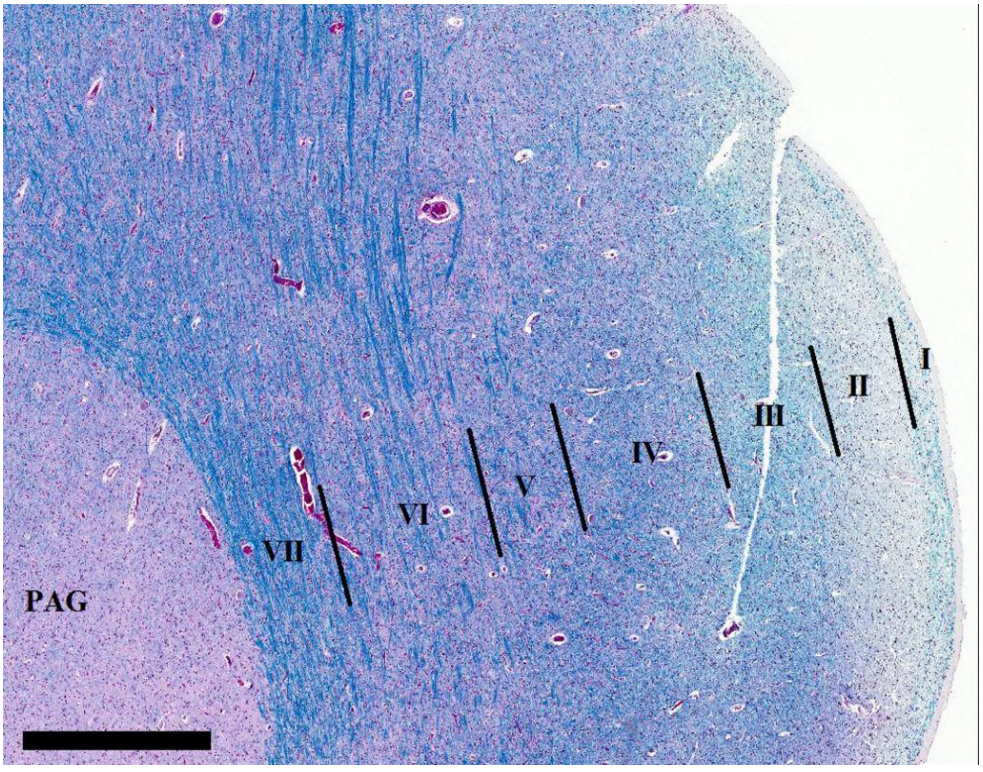

Fig 2. Pathology in the superior colliculus (SC) of a case of chronic traumatic encephalopathy (CTE) showing tau-immunoreactive pathology predominantly in lower laminae. Arrow head = neurofibrillary tangle (NFT), Arrow = Grain, Star = dystrophic neurite (DN); Phosphorylated tau (AT8) immunohistochemistry, bar = 20 μm).

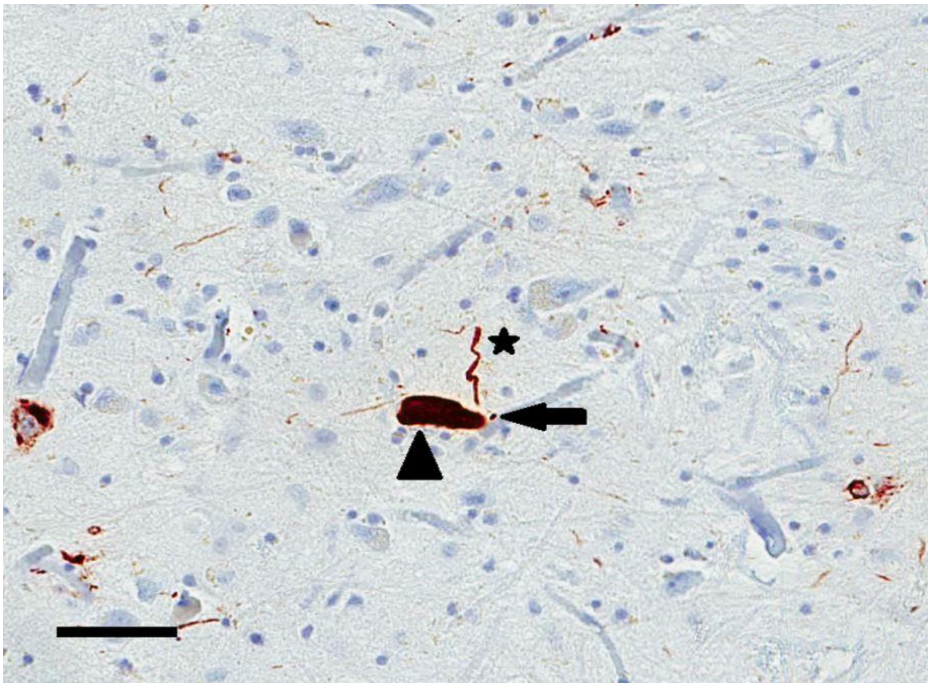

Fig 3. The overall abundance of tau-immunoreactive pathology (brown immunostaining) in the superior colliculus (SC) of each case (cases A to E) of chronic traumatic encephalopathy (CTE) and in a control case; Phosphorylated tau (AT8) immunohistochemistry, bars = 300 μm).

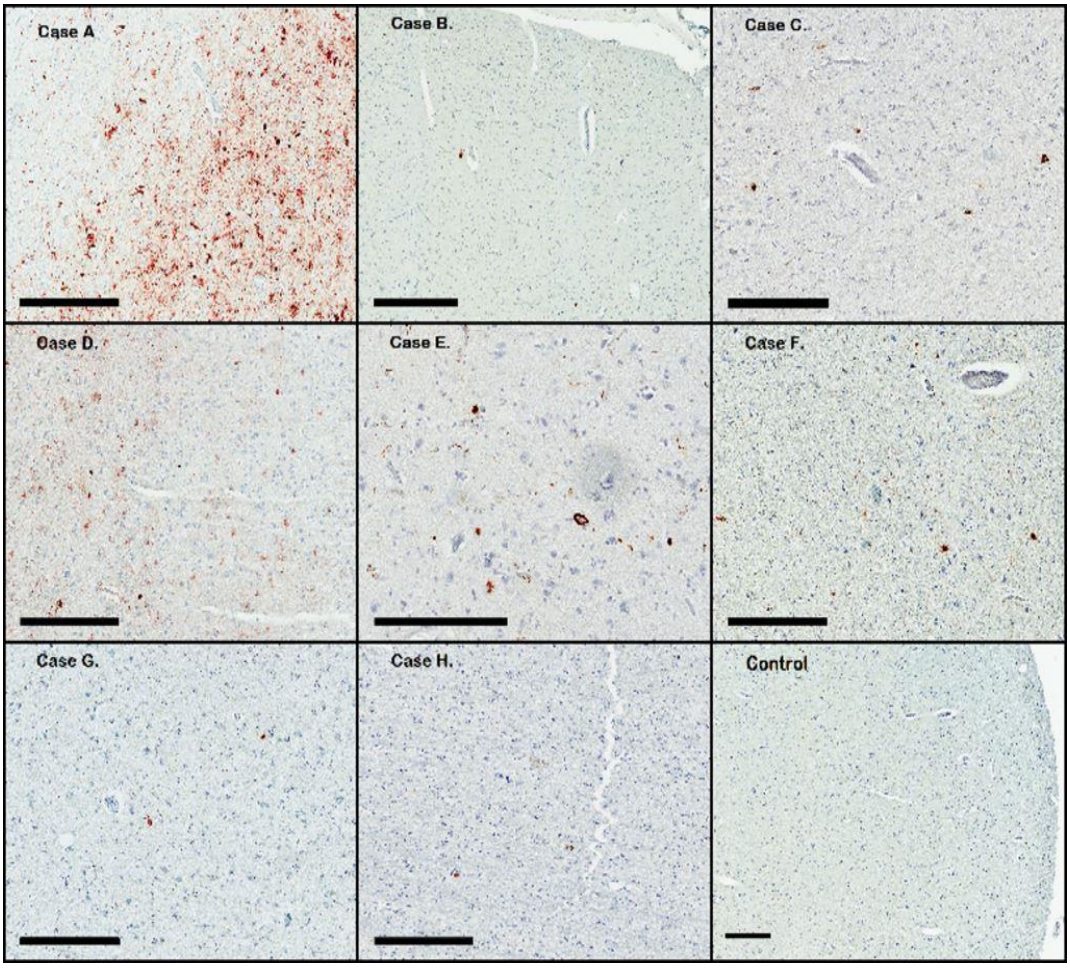

Fig 4. Mean densities of histological features (NFT = Neurofibrillary tangles, NT = neuropil threads, GR = Grains, AT = Astrocytic tangles, EN = Enlarged neurons, N = Neurons, V = Vacuoles, BV = Blood vessels) in the superior colliculus (SC) of control and cases of chronic traumatic encephalopathy (CTE). Comparison of CTE and control cases: NFT $t = 2.28$ ($P > 0.05$), NT $t = 1.13$, $P > 0.05$, DLG $t = 1.66$, $P > 0.05$, AT $t = 1.87$, $P > 0.05$), EN $t = 0.54$ ($P > 0.05$), vacuoles $t = 0.92$ ($P > 0.05$), blood vessel contacts $t = 0.35$ ($P > 0.05$), Neurons $t = 3.82$ ($P < 0.01$).

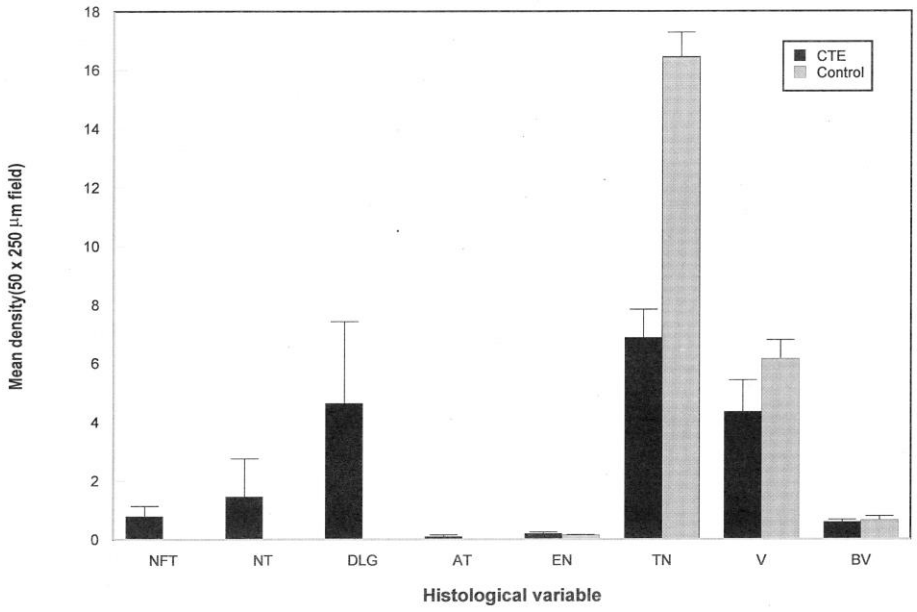

Fig 5. The distribution of the surviving neurons across the superior colliculus (SC) in a control brain and a case of chronic traumatic encephalopathy (CTE) (Case G). In both cases, variation in density of neurons with distance across the SC was fitted by a third-order (cubic) polynomial.

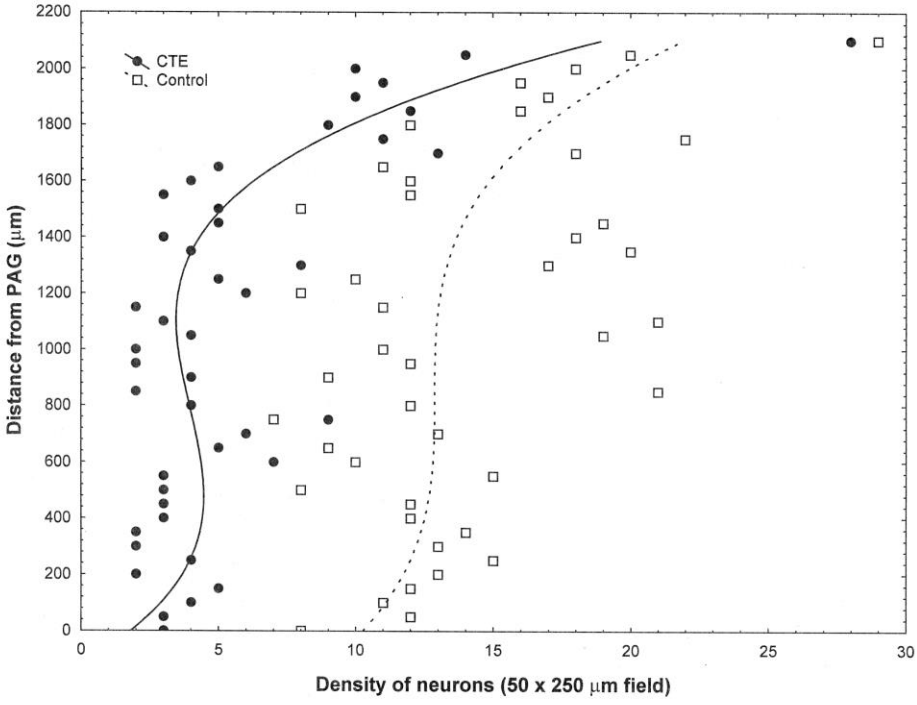

Fig 6. Input and output connections of the various laminae of the superior colliculus (SC) (LGN = Lateral geniculate nucleus). Based on Brodal[41]